

Exact trace formulas for two-dimensional electron magnetism

J. P. Gazeau,^{1,*} P. Y. Hsiao,^{1,†} and A. Jellal^{2,‡}

¹*Laboratoire de Physique Théorique de la Matière Condensée, Case 7020, Université Paris 7 Denis Diderot, 2 Place Jussieu, 75251 Paris Cedex 05, France*

²*Laboratory of High Energy Physics, Faculty of Sciences, Ibn Battouta Street, P.O. Box 1014, Rabat, Morocco*

(Received 22 December 2000; revised manuscript received 6 June 2001; published 19 February 2002)

We study in this paper the possible occurrence of orbital magnetism for two-dimensional electrons confined by a harmonic potential in various regimes of temperature and magnetic field. We give exact expressions for the thermodynamical potential, the magnetic moment, and the average number of electrons. The derivation of involved trace formulas is based on residue series in the complex plane. The results yield a full description of the phase diagram of the magnetization.

DOI: 10.1103/PhysRevB.65.094427

PACS number(s): 75.20.-g, 71.10.Ca, 75.30.Kz

I. INTRODUCTION

In a recent paper, Ishikawa and Fukuyama¹ describe the possible orbital magnetism for two-dimensional electrons confined by a harmonic potential and submitted to a constant normal magnetic field (the so-called Fock-Darwin model²). By exploring various regimes of temperature and magnetic field, they afford a quite large complement of information in regard to a previous paper³ devoted to the same subject. According to the range of values assumed by the relative ratios between the three characteristic energy scales present in the model, namely the thermodynamical unit $k_B T$, the magnetic quantum $\hbar \omega_c$, and the harmonic quantum $\hbar \omega_0$, they explain the existence of the different magnetic regimes. As a matter of fact, they distinguish between the “mesoscopic fluctuation” regime [$k_B T \lesssim \hbar(\sqrt{\omega_c^2 + 4\omega_0^2} - \omega_c)/2 \equiv \hbar \omega_-$], the “Landau diamagnetism” regime [$k_B T \gtrsim \hbar(\sqrt{\omega_c^2 + 4\omega_0^2} + \omega_c)/2 \equiv \hbar \omega_+$], and the “de Haas-van Alphen” regime. Their studies rest upon an approximate expression for the thermodynamical potential Ω which is derived from a standard Poisson summation formula and from which they are able to get the magnetic moment.

We present in this paper expressions for the thermodynamical potential and the magnetic moment for the above model. Our expressions are exact, in contrast to those in Ref. 1, and our results yield a full description of the phase diagram of the magnetization. Our derivation crucially rests upon the observation that the Fermi-Dirac function is a fixed point of the Fourier transform. Exact series expansions ensue by simple application of the residue theorem. Our results for the thermodynamical potential, the orbital magnetic moment, the subsequent magnetic susceptibility, and the average number of electrons are easily tractable and analyzable.

Since the pioneering work of Landau in 1930, orbital magnetism of electron gases has been the subject of considerable attention, especially during the last decades with the advent of experimental opportunities, more precisely with the availability of two-dimensional electronic devices, quantum boxes, or mesoscopic finite-size objects. One can find in Refs. 4 or 5 a good account of recent theoretical investigations on the subject, especially from a semiclassical point of view.

In the next section, we shall give a short review of the Fock-Darwin problem. The eigenvalues of the Hamiltonian will be derived through an algebraic approach. In Secs. III we establish the exact trace formulas for the thermodynamical potential. In Sec. IV, the magnetic moment and the average number of electrons are calculated. We discuss their behavior in different temperature and magnetic-field regions. In the conclusion we give some remarks and comments on the possible extension of our approach to other systems of physical interest.

II. HAMILTONIAN AND ITS EIGENVALUES

The Hamiltonian for two-dimensional spinless electrons confined by an isotropic harmonic potential and submitted to a constant perpendicular magnetic field is written as

$$\mathcal{H} = \frac{1}{2m_e} \left(\mathbf{P} + \frac{e}{c} \mathbf{A} \right)^2 + \frac{1}{2} m_e \omega_0^2 \mathbf{R}^2, \quad (2.1)$$

where Coulomb interactions are neglected and the symmetric gauge $\mathbf{A} = \frac{1}{2} \mathbf{H} \times \mathbf{R}$ will be applied in our studies. The classical radius R_m of the system is classically defined as

$$\frac{1}{2} m \omega_0^2 R_m^2 = \mu, \quad (2.2)$$

where μ is the chemical potential of the considered electron gas. The Hamiltonian can be solved by the following algebraic approach in which two bosonic annihilation operators a_d and a_g are introduced:

$$a_d = \frac{1}{2} \left[\left(\frac{X}{l_0} + \frac{l_0}{\hbar} P_y \right) + i \left(-\frac{Y}{l_0} + \frac{l_0}{\hbar} P_x \right) \right], \quad (2.3)$$

$$a_g = \frac{1}{2} \left[\left(\frac{X}{l_0} - \frac{l_0}{\hbar} P_y \right) + i \left(\frac{Y}{l_0} + \frac{l_0}{\hbar} P_x \right) \right], \quad (2.4)$$

where $l_0 = \sqrt{2\hbar/m\omega}$. We define the number operators $N_d = a_d^\dagger a_d$ and $N_g = a_g^\dagger a_g$. The Hamiltonian is split into the sum of two independent harmonic oscillators and written as

$$\mathcal{H} = \hbar \omega_+ \left(N_d + \frac{1}{2} \right) + \hbar \omega_- \left(N_g + \frac{1}{2} \right), \quad (2.5)$$

where ω_c is the cyclotron frequency eH/mc , $w = \sqrt{\omega_c^2 + 4\omega_0^2}$, and $\omega_{\pm} = (\omega \pm \omega_c)/2$. The eigenvalues of the Hamiltonian hence read as

$$E_{n_d n_g} = \hbar \omega_+ \left(n_d + \frac{1}{2} \right) + \hbar \omega_- \left(n_g + \frac{1}{2} \right), \quad (2.6)$$

where the quantum numbers n_d and n_g are non-negative integers.

III. THERMODYNAMICAL POTENTIAL

We will work in a grand canonical ensemble. In Fermi-Dirac statistics the thermodynamical potential is given by

$$\Omega = -\frac{1}{\beta} \text{Tr} \log(1 + e^{-\beta(\mathcal{H}-\mu)}) \quad (3.1)$$

with $\beta = 1/(k_B T)$. The magnetic moment M is calculated by taking the derivative of $-\Omega$ with respect to the magnetic field H and it yields

$$M = -\left(\frac{\partial \Omega}{\partial H} \right)_{\mu} = -\frac{2\mu_B}{\omega} \text{Tr} \frac{(N_d + 1/2)\omega_+ - (N_g + 1/2)\omega_-}{1 + e^{\beta(\mathcal{H}-\mu)}} \quad (3.2)$$

$$= -\frac{2\mu_B}{\omega} \sum_{n_d=0}^{\infty} \sum_{n_g=0}^{\infty} \frac{(n_d + 1/2)\omega_+ - (n_g + 1/2)\omega_-}{1 + e^{\beta\hbar(\omega_+ n_d + \omega_- n_g + \omega/2) - \beta\mu}}, \quad (3.3)$$

where $\mu_B = \hbar e/(2mc)$ is the Bohr magneton. The average number of electrons is given by taking the derivative of $-\Omega$ with respect to the chemical potential μ :

$$\langle N_e \rangle = -\left(\frac{\partial \Omega}{\partial \mu} \right) \quad (3.4)$$

$$= \text{Tr} f(\mathcal{H}) = \sum_{n_d=0}^{\infty} \sum_{n_g=0}^{\infty} f(E_{n_d n_g}), \quad (3.5)$$

where $f(E) = 1/(1 + e^{\beta(E-\mu)})$ is the Fermi-Dirac distribution. Despite their concise appearance, the computation of the double series in Eq. (3.3) and in Eq. (3.5) is not easily tractable on a numerical level. Fortunately, the complete integrability of the model allows us to give this double series a simpler form. In the next subsection we will present general trace formulas which allow us to give a more appropriate form to the physical quantities Ω , M , and $\langle N_e \rangle$.

A. Fermi-Dirac trace formulas

It is well known that, like the Gaussian function, the function $\text{sech}x = 1/\cosh x$ is a fixed point for the Fourier transform in the Schwartz space:

$$\frac{1}{\cosh \sqrt{\frac{\pi}{2}}x} = \frac{1}{\sqrt{2}\pi} \int_{-\infty}^{+\infty} \frac{e^{-ixy}}{\cosh \sqrt{\frac{\pi}{2}}y} dy. \quad (3.6)$$

Hence, for a Hamiltonian \mathcal{H} , we can write for the corresponding Fermi-Dirac operator

$$f(\mathcal{H}) \equiv \frac{1}{1 + e^{\beta(\mathcal{H}-\mu)}} = \int_{-\infty}^{+\infty} \frac{e^{-(ik+1)(\beta/2)(\mathcal{H}-\mu)}}{4 \cosh \frac{\pi}{2}k} dk. \quad (3.7)$$

Similarly, we can write for the thermodynamical potential operator

$$-\frac{1}{\beta} \ln(1 + e^{-\beta(\mathcal{H}-\mu)}) = -\frac{1}{\beta} \int_{-\infty}^{+\infty} \frac{e^{-(ik+1)(\beta/2)(\mathcal{H}-\mu)}}{\left(2 \cosh \frac{\pi}{2}k\right)(ik+1)} dk. \quad (3.8)$$

Therefore, the average number of fermions and the thermodynamical potential can be written (at least formally) as follows:

$$\langle N \rangle = \text{Tr} f(\mathcal{H}) = \int_{-\infty}^{+\infty} \frac{e^{(ik+1)\beta\mu/2}}{4 \cosh \frac{\pi}{2}k} \Theta(k) dk, \quad (3.9)$$

$$\begin{aligned} \Omega &= \text{Tr} \left(-\frac{1}{\beta} \ln(1 + e^{-\beta(\mathcal{H}-\mu)}) \right) \\ &= -\frac{1}{\beta} \int_{-\infty}^{+\infty} \frac{e^{(ik+1)\beta\mu/2}}{\left(2 \cosh \frac{\pi}{2}k\right)(ik+1)} \Theta(k) dk, \end{aligned} \quad (3.10)$$

where Θ designates the function

$$\Theta(k) = \text{Tr}(e^{-(ik+1)(\beta/2)\mathcal{H}}). \quad (3.11)$$

Observe that $(2m+1)i$, $m \in \mathbb{Z}$ are (simple) poles for the function $1/\cosh(\pi/2)k$ and i is a pole for the functions $\Theta(k)$ and $1/(ik+1)$. These Fourier integrals can be evaluated by using residue theorems if the integrand functions $\Phi_1(k) = \Theta(k)/\cosh(\pi/2)k$ and $\Phi_2(k) = \Theta(k)/[(ik+1)\cosh(\pi/2)k]$ satisfy the Jordan lemma, that is, $\Phi_1(Re^{i\theta}) \leq g(R)$, $\Phi_2(Re^{i\theta}) \leq h(R)$, for all $\theta \in [0, \pi]$, and $g(R)$ and $h(R)$ vanish as $R \rightarrow \infty$. The quantities $\langle N \rangle$ and Ω are then formally given by

$$2\pi i \left[a_{-1}(i) + \sum_{m=1}^{\infty} a_{-1}[(2m+1)i] + \sum_{\nu} a_{-1}(k_{\nu}) \right], \quad (3.12)$$

where $a_{-1}(\dots)$ denotes the residue of the involved integrand at pole (\dots) , and the k_{ν} 's are the poles (with the exclusion of the pole i) of $\Theta(k)$ in the complex k plane.

B. Exact expressions for the thermodynamical potential

We now determine the thermodynamical potential in a precise way by applying the formulas (3.10) and (3.12) to our Hamiltonian given in Eq. (2.5). The function $\Theta(k)$ defined by Eq. (3.11) takes the following closed form:

$$\begin{aligned}
 \Theta(k) &= \text{Tr}(e^{-(ik+1)(\beta/2)\mathcal{H}}) \\
 &= e^{-(ik+1)(\beta/4)\hbar\omega} \frac{1}{1 - e^{-(ik+1)(\beta/2)\hbar\omega_+}} \\
 &\quad \times \frac{1}{1 - e^{-(ik+1)(\beta/2)\hbar\omega_-}}. \quad (3.13)
 \end{aligned}$$

The Fourier integral representation for the thermodynamical potential consequently reads as

$$\begin{aligned}
 \Omega &= -\frac{1}{\beta} \int_{-\infty}^{+\infty} \frac{e^{-(ik+1)\beta/2[(\hbar\omega/2)-\mu]}}{2 \cosh \frac{\pi}{2}k} \left(\frac{1}{ik+1} \right) \\
 &\quad \times \left(\frac{1}{1 - e^{-(ik+1)(\beta/2)\hbar\omega_+}} \right) \left(\frac{1}{1 - e^{-(ik+1)(\beta/2)\hbar\omega_-}} \right) dk. \quad (3.14)
 \end{aligned}$$

As indicated in the formula (3.11), this Fourier integral is given as a series by using the residue theorem. One can easily see that the numbers $(2m+1)i$, $m \in \mathbb{Z}$ are simple poles of $\text{sech}(\pi/2)k$, i is a double pole of $\Theta(k)$, and $i + 4\pi m/(\beta\hbar\omega_+)$, $i + 4\pi m/(\beta\hbar\omega_-)$, and $m \in \mathbb{Z}^*$ are simple or double poles of $\Theta(k)$ according to whether or not ω_+ and ω_- are uncommensurable (see Fig. 1). In order to fulfill the requirements of the Jordan lemma, one has to consider the following two cases: $\mu \leq \hbar\omega/2$ and $\mu \geq \hbar\omega/2$. In the first case we take an integration path lying in the lower half-plane and involving only the simple poles $(2m+1)i$, $m < 0$. It leads to the result

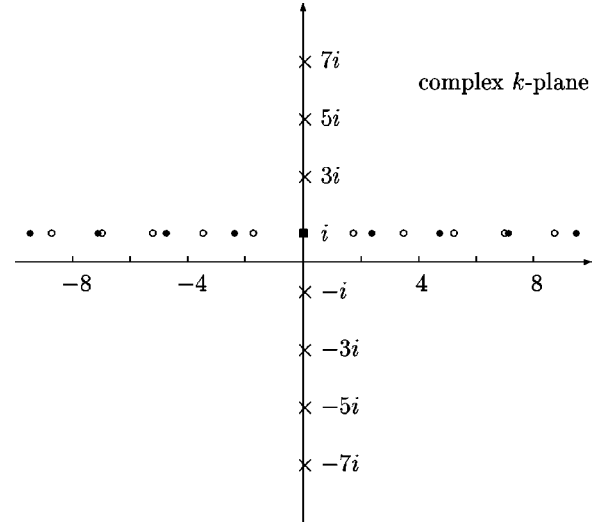


FIG. 1. Poles of the Fourier representation of the thermodynamical potential Ω . The poles lying on the imaginary axis are simple except for the point i which is of order 4. The poles lying on the line $k=i$ in the complex k plane (i is excluded) may be simple or double depending on whether or not ω_+ and ω_- are uncommensurable.

$$\Omega = \frac{1}{4\beta} \sum_{m=1}^{\infty} \frac{(-1)^m}{m} \frac{e^{\beta\mu m}}{\sinh\left(\frac{\beta}{2}\hbar\omega_+ m\right) \sinh\left(\frac{\beta}{2}\hbar\omega_- m\right)}. \quad (3.15)$$

In the second case, an integration path in the upper half-plane is chosen. It encircles all the other poles: $(2m+1)i$, $m \geq 0$, $i + 4\pi m/(\beta\hbar\omega_+)$, $i + 4\pi m/(\beta\hbar\omega_-)$, and $m \in \mathbb{Z}^*$, as shown in Fig. 1. We present the result in a manner which will render apparent the various regimes:

$$\begin{aligned}
 \Omega &= \underbrace{(\Omega_L + \Omega_{01})}_{= 2\pi i} + \underbrace{\Omega_{02}}_{\sum_{m \geq 1} a_{-1}[(2m+1)i]} + \underbrace{\Omega_{\text{osc}}}_{\sum_{m \neq 0} \left[a_{-1} \left(i + \frac{4\pi}{\beta\hbar\omega_{\pm}} m_{\pm} \right) \right]}. \quad (3.16)
 \end{aligned}$$

The first term is at the origin of the Landau diamagnetism:

$$\Omega_L = \frac{\mu}{24} \left(\frac{\omega_c}{\omega_0} \right)^2 = -\frac{1}{2} \chi_L H^2, \quad (3.17)$$

where $\chi_L = -\frac{1}{3} \mu (\mu_B / \hbar \omega_0)^2 \equiv -\frac{1}{3} D_0 \mu_B^2$ is the Landau diamagnetic susceptibility. The coefficient $D_0 = \mu / (\hbar \omega_0)^2$ can be interpreted as the density of states at Fermi energy. The second term, which gives no contribution to the magnetization, is written as

$$\Omega_{01} = -\frac{\mu}{6} \left[\left(\frac{\mu}{\hbar \omega_0} \right)^2 + \pi^2 \left(\frac{k_B T}{\hbar \omega_0} \right)^2 - \frac{1}{2} \right]. \quad (3.18)$$

The third term is given as

$$\Omega_{02} = \frac{1}{4\beta} \sum_{m=1}^{\infty} \frac{(-1)^m}{m} \frac{\exp\left(-\frac{\mu}{k_B T} m\right)}{\sinh\left(\frac{\hbar\omega_+}{2k_B T} m\right) \sinh\left(\frac{\hbar\omega_-}{2k_B T} m\right)}. \quad (3.19)$$

It becomes negligible at a low-temperature regime $k_B T \ll \mu$. The last term Ω_{osc} is responsible for the oscillatory behavior. We need to distinguish between irrational values of ω_+ / ω_- and rational ones.

For the case $\omega_+/\omega_- \notin \mathbb{Q}$,

$$\Omega_{\text{osc}} = \frac{1}{2\beta} \sum_{m=1}^{\infty} \frac{(-1)^m}{m} \left[\frac{\sin\left(\frac{2\mu}{\hbar\omega_-} \pi m\right)}{\sin\left(\frac{\omega_+}{\omega_-} \pi m\right) \sinh\left(\frac{2k_B T}{\hbar\omega_-} \pi^2 m\right)} + \frac{\sin\left(\frac{2\mu}{\hbar\omega_+} \pi m\right)}{\sin\left(\frac{\omega_-}{\omega_+} \pi m\right) \sinh\left(\frac{2k_B T}{\hbar\omega_+} \pi^2 m\right)} \right] \equiv \Omega_{\text{osc}}^- + \Omega_{\text{osc}}^+. \quad (3.20)$$

For the case $\omega_+/\omega_- = p/q \in \mathbb{Q}$, $\gcd(p, q) = 1$, $\omega_+/p = \omega_-/q = 2l/(\hbar\beta) \in \mathbb{R}$,

$$\begin{aligned} \Omega_{\text{osc}} = \frac{1}{2\beta} & \left[\sum_{m=1, m \neq 0 \pmod q}^{\infty} \frac{(-1)^m}{m} \frac{\sin\left(\frac{2\mu}{\hbar\omega_-} \pi m\right)}{\sin\left(\frac{\omega_+}{\omega_-} \pi m\right) \sinh\left(\frac{2k_B T}{\hbar\omega_-} \pi^2 m\right)} \right. \\ & + \sum_{m=1, m \neq 0 \pmod p}^{\infty} \frac{(-1)^m}{m} \frac{\sin\left(\frac{2\mu}{\hbar\omega_+} \pi m\right)}{\sin\left(\frac{\omega_-}{\omega_+} \pi m\right) \sinh\left(\frac{2k_B T}{\hbar\omega_+} \pi^2 m\right)} \\ & \left. + \frac{1}{lpq} \sum_{k=1}^{\infty} \frac{(-1)^{(p+q)k}}{k \sinh\left(\frac{\pi^2}{l} k\right)} \left\{ \frac{\mu}{k_B T} \cos\left(\frac{\mu \pi k}{k_B T l}\right) - \left[\pi \coth\left(\frac{\pi^2}{l} k\right) + \frac{l}{\pi k} \right] \sin\left(\frac{\mu \pi k}{k_B T l}\right) \right\} \right]. \quad (3.21) \end{aligned}$$

IV. AVERAGE NUMBER OF ELECTRONS AND MAGNETIC MOMENT

In this section, we will exploit the formulas (3.15)–(3.21) to obtain the exact expressions of the average number of electrons and the magnetization. We will restrict ourselves to the more realistic case $\mu \geq \hbar\omega/2$.

The average number of electrons is easily derived from Eq. (3.4) and is found to be

$$\begin{aligned} \langle N_e \rangle = & -\frac{1}{24} \left(\frac{\omega_c}{\omega_0} \right)^2 + \frac{1}{2} \left[\left(\frac{\mu}{\hbar\omega_0} \right)^2 + \frac{\pi^2}{3} \left(\frac{k_B T}{\hbar\omega_0} \right)^2 - \frac{1}{6} \right] + \frac{1}{4} \sum_{m=1}^{\infty} (-1)^m \frac{e^{-\beta\mu m}}{\sinh\left(\frac{\beta}{2} \hbar\omega_+ m\right) \sinh\left(\frac{\beta}{2} \hbar\omega_- m\right)} \\ & - \pi \sum_{m=1}^{\infty} (-1)^m \left[\frac{k_B T}{\hbar\omega_-} \frac{\cos\left(\frac{2\mu}{\hbar\omega_-} \pi m\right)}{\sin\left(\frac{\omega_+}{\omega_-} \pi m\right) \sinh\left(\frac{2k_B T}{\hbar\omega_-} \pi^2 m\right)} + \frac{k_B T}{\hbar\omega_+} \frac{\cos\left(\frac{2\mu}{\hbar\omega_+} \pi m\right)}{\sin\left(\frac{\omega_-}{\omega_+} \pi m\right) \sinh\left(\frac{2k_B T}{\hbar\omega_+} \pi^2 m\right)} \right] \\ \equiv & \langle N_e \rangle_L + \langle N_e \rangle_{01} + \langle N_e \rangle_{02} + \langle N_e \rangle_{\text{osc}}^- + \langle N_e \rangle_{\text{osc}}^+, \quad (4.1) \end{aligned}$$

where we suppose that ω_+ and ω_- are uncommensurable.

The magnetic moment is decomposed into four parts and is expressed in Bohr magneton units:

$$M = \chi_L H - 2\mu_B \left(\frac{\partial \Omega_{02}}{\partial \hbar\omega_c} \right)_{\mu} - 2\mu_B \left(\frac{\partial \Omega_{\text{osc}}}{\partial \hbar\omega_c} \right)_{\mu} \equiv 2\mu_B (\mathcal{M}_L + \mathcal{M}_0 + \mathcal{M}_{\text{osc}}^- + \mathcal{M}_{\text{osc}}^+), \quad (4.2)$$

where

$$\mathcal{M}_L = \frac{-\mu}{12\hbar\omega_0} \left(\frac{\omega_c}{\omega_0} \right) \equiv \frac{1}{2\mu_B} \chi_L H, \quad (4.3)$$

$$\mathcal{M}_0 = \frac{1}{8\omega} \sum_{m=1}^{\infty} (-1)^m e^{-\beta\mu m} \frac{[\omega_+ \coth(\beta\hbar\omega_+ m/2) - \omega_- \coth(\beta\hbar\omega_- m/2)]}{\sinh(\beta\hbar\omega_+ m/2) \sinh(\beta\hbar\omega_- m/2)}, \quad (4.4)$$

and, for the irrational case $\omega_+/\omega_- \notin \mathbb{Q}$,

$$\mathcal{M}_{\text{osc}}^- = -\frac{k_B T}{\hbar \omega_-} \sum_{m=1}^{\infty} \frac{(-1)^m \sin[2\pi m \mu / (\hbar \omega_-)]}{\sin(\pi m \omega_+ / \omega_-) \sinh[2\pi^2 m k_B T / (\hbar \omega_-)]} \times \left[\frac{\pi \mu}{\hbar \omega_-} \cot\left(2\pi m \frac{\mu}{\hbar \omega_-}\right) - \frac{\pi \omega_+}{\omega_-} \cot\left(\pi m \frac{\omega_+}{\omega_-}\right) - \frac{\pi^2 k_B T}{\hbar \omega_-} \coth\left(2\pi^2 m \frac{k_B T}{\hbar \omega_-}\right) \right], \quad (4.5)$$

$$\mathcal{M}_{\text{osc}}^+ = \frac{k_B T}{\hbar \omega_+} \sum_{m=1}^{\infty} \frac{(-1)^m \sin[2\pi m \mu / (\hbar \omega_+)]}{\sin(\pi m \omega_- / \omega_+) \sinh[2\pi^2 m k_B T / (\hbar \omega_+)]} \times \left[\frac{\pi \mu}{\hbar \omega_+} \cot\left(2\pi m \frac{\mu}{\hbar \omega_+}\right) - \frac{\pi \omega_-}{\omega_+} \cot\left(\pi m \frac{\omega_-}{\omega_+}\right) - \frac{\pi^2 k_B T}{\hbar \omega_+} \coth\left(2\pi^2 m \frac{k_B T}{\hbar \omega_+}\right) \right]. \quad (4.6)$$

We will not give the expressions of $\mathcal{M}_{\text{osc}}^{\pm}$ in the rational case because the magnetization is a continuous function of ω_c and its behavior can be fully understood from the irrational one.

V. DISCUSSION

The temperature scale is compared to the two natural modes ω_{\pm} of the system and draws three possible intrinsic regimes: the high-temperature regime $k_B T > \hbar \omega_+$, the low-temperature regime $k_B T < \hbar \omega_-$, and the intermediate-temperature regime $\hbar \omega_- < k_B T < \hbar \omega_+$. Remember that we work in the large electron number region $\mu > \hbar \omega/2$.

A. High-temperature regime: $k_B T > \hbar \omega_+ > \hbar \omega_-$

This inequality implies the following constraint on the field:

$$\frac{\omega_c}{\omega_0} < \frac{k_B T}{\hbar \omega_0} - \frac{\hbar \omega_0}{k_B T} \approx \frac{k_B T}{\hbar \omega_0}. \quad (5.1)$$

We can see that \mathcal{M}_0 is the dominant term for the magnetic moment in regard to \mathcal{M}_{osc} because of the smallness of arguments of the sinh (in the denominator) and coth (in the numerator) functions. Hence, $M \approx 2\mu_B(\mathcal{M}_L + \mathcal{M}_0)$, which shows mainly Landau diamagnetism. Similarly, we infer from Eq. (4.1) that $\langle N_e \rangle \approx \langle N_e \rangle_L + \langle N_e \rangle_{01} + \langle N_e \rangle_{02}$.

B. Low-temperature regime: $k_B T < \hbar \omega_-$

The magnetic field is restricted by the inequality

$$\frac{\omega_c}{\omega_0} < \frac{\hbar \omega_0}{k_B T} - \frac{k_B T}{\hbar \omega_0} \approx \frac{\hbar \omega_0}{k_B T}. \quad (5.2)$$

Now the \mathcal{M}_0 term becomes excessively small due to the rapidly decreasing exponential factor and the large arguments of the hyperbolic functions present in the expression. The magnetization is hence approximately determined by the three terms \mathcal{M}_L , $\mathcal{M}_{\text{osc}}^+$, and $\mathcal{M}_{\text{osc}}^-$ and exhibits oscillating behavior.

1. Strong fields $\omega_c \gg \omega_0$

We make the following approximations:

$$\omega_+ \approx \omega_c \left[1 + \left(\frac{\omega_0}{\omega_c} \right)^2 \right], \quad \omega_- \approx \frac{\omega_0^2}{\omega_c}, \quad \frac{\omega_+}{\omega_-} \approx \left(\frac{\omega_c}{\omega_0} \right)^2. \quad (5.3)$$

We assume also that $\omega_c \leq 2\omega_0 \sqrt{(\mu/\hbar)^2 - 1}$ to ensure the validity of $\mu \geq \hbar \omega/2$. One can see that the denominator of $\mathcal{M}_{\text{osc}}^+$ contains the product of sin and two sinh's with a small argument and, hence, $M \approx 2\mu_B(\mathcal{M}_L + \mathcal{M}_{\text{osc}}^+)$. In particular, after replacing ω_+ by ω_c in the sinus argument of the numerator of $\mathcal{M}_{\text{osc}}^+$, we find that the magnetization is periodic with respect to the inverse of the magnetic field, a characteristic fact of the ‘‘de Haas–van Alphen’’ regime. A similar behavior holds for the electron number $\langle N_e \rangle \approx \langle N_e \rangle_L + (\mu/\hbar \omega_0)^2/2 + \langle N_e \rangle_{\text{osc}}^+$.

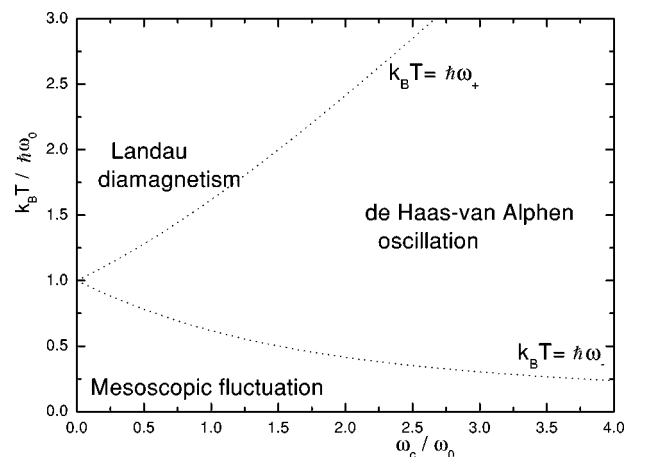


FIG. 2. Qualitative phase diagram of the magnetization. In a high-temperature and low magnetic-field region, the system shows Landau diamagnetism; in a low-temperature and low magnetic-field region, mesoscopic fluctuations appear; and in a strong magnetic-field region, the system experiences the de Haas–van Alphen oscillation phase. The two curves, $k_B T = \hbar \omega_+$ and $k_B T = \hbar \omega_-$, give a qualitative indication about the phase borders.

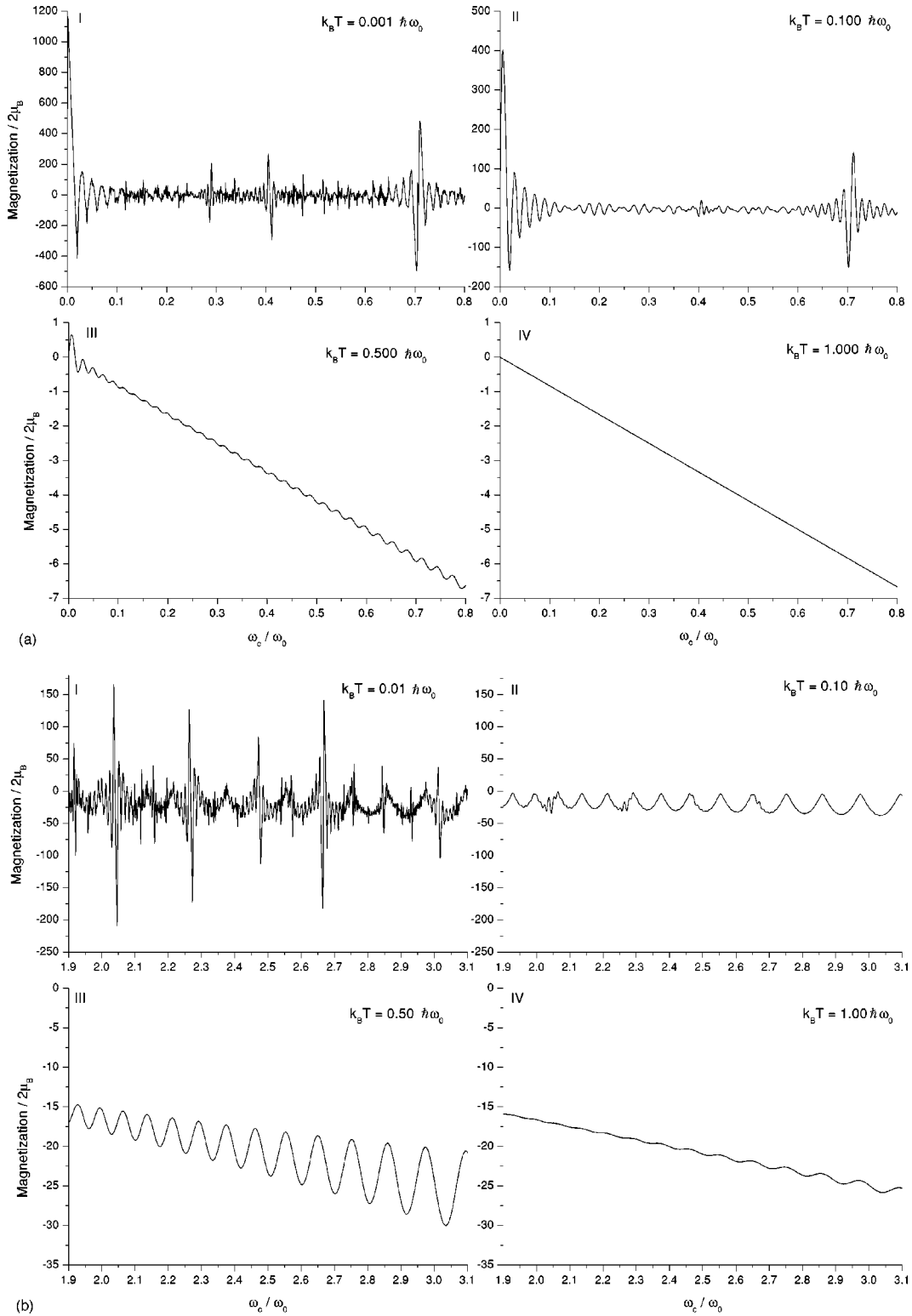


FIG. 3. Magnetization curves versus the magnetic field at different temperatures. We represent the cyclotron frequency in ω_0 units and the magnetization in $2\mu_B$ units. The chemical potential μ is set up at $100.0\hbar\omega_0$. (a) ω_c is less than $0.8\omega_0$. Temperatures are chosen to be (i) $0.001\hbar\omega_0$, (ii) $0.1\hbar\omega_0$, (iii) $0.5\hbar\omega_0$, and (iv) $1.0\hbar\omega_0$, respectively. Please note different scales are used for the magnetization axes. (b) ω_c is between $1.9\omega_0$ and $3.1\omega_0$. Temperatures are chosen to be (i) $0.01\hbar\omega_0$, (ii) $0.1\hbar\omega_0$, (iii) $0.5\hbar\omega_0$, and (iv) $1.0\hbar\omega_0$, respectively. (c) ω_c is between $4.0\omega_0$ and $15.0\omega_0$. Temperatures are chosen to be (i) $0.1\hbar\omega_0$, (ii) $0.5\hbar\omega_0$, (iii) $1.0\hbar\omega_0$, and (iv) $5.0\hbar\omega_0$, respectively. (d) ω_c is greater than $15.0\omega_0$. Temperatures are chosen to be (i) $0.001\hbar\omega_0$, (ii) $0.5\hbar\omega_0$, (iii) $1.0\hbar\omega_0$, and (iv) $5.0\hbar\omega_0$, respectively. Please note the scales of the axes of (i) are enlarged in order to show the detail of the magnetization curve. We can see that mesoscopic fluctuations mix with the de Haas–van Alphen oscillation in extreme low temperature $0.001\hbar\omega_0$.

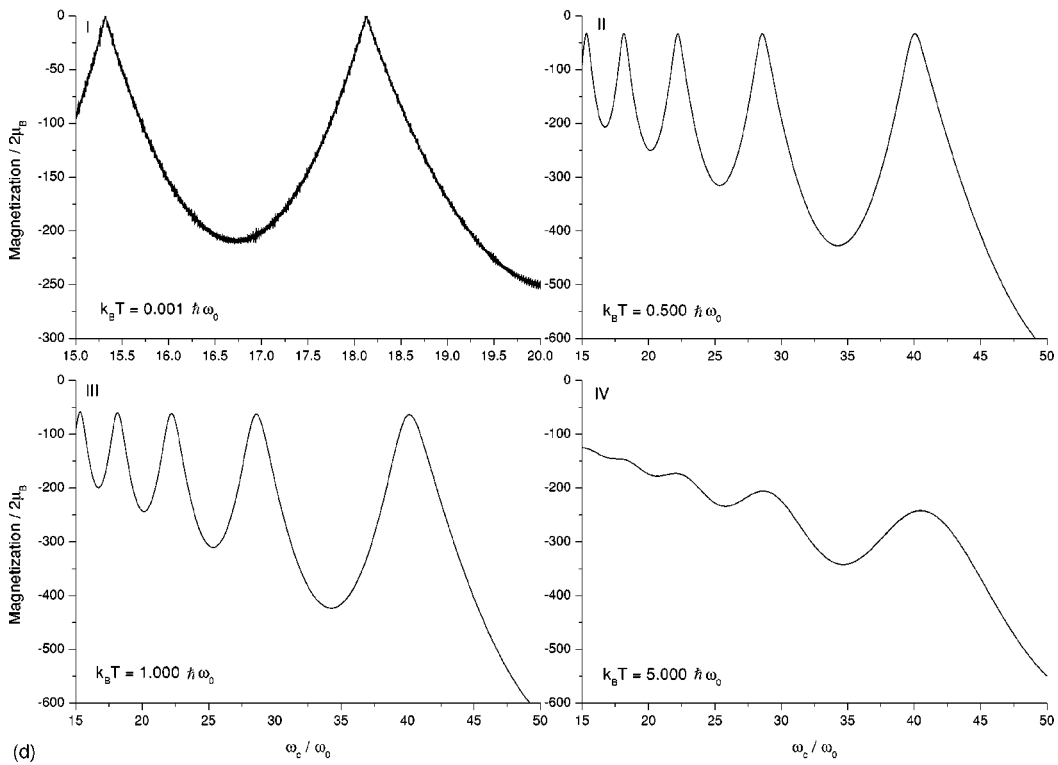
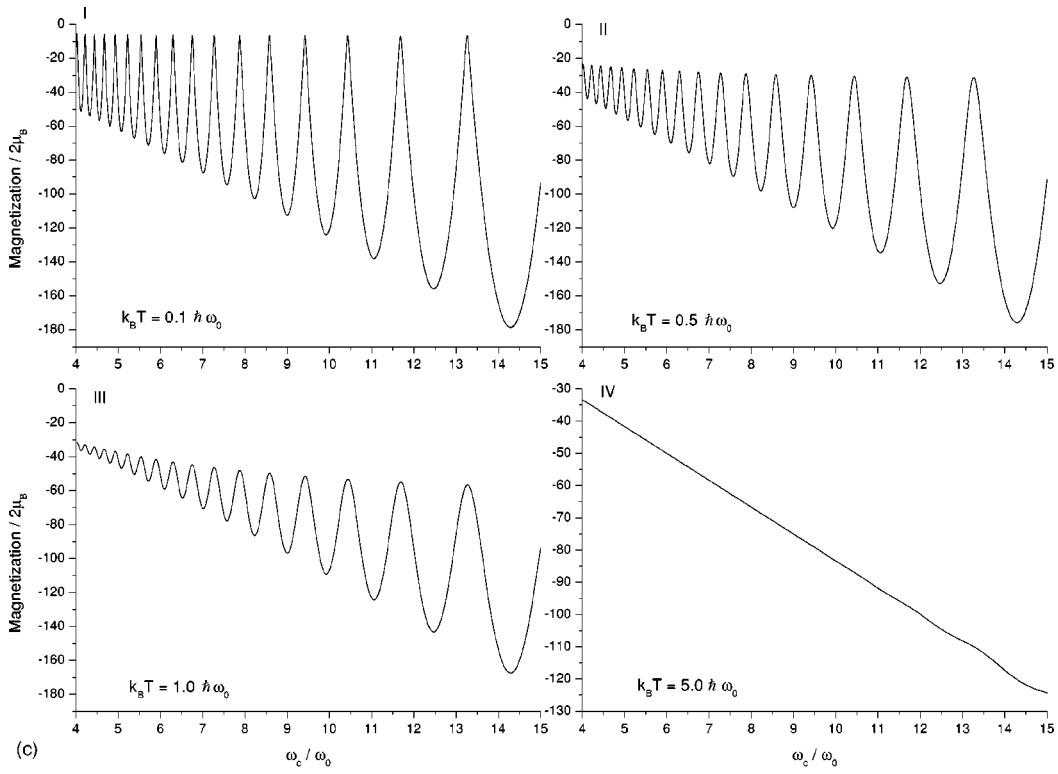


FIG. 3. (Continued.)

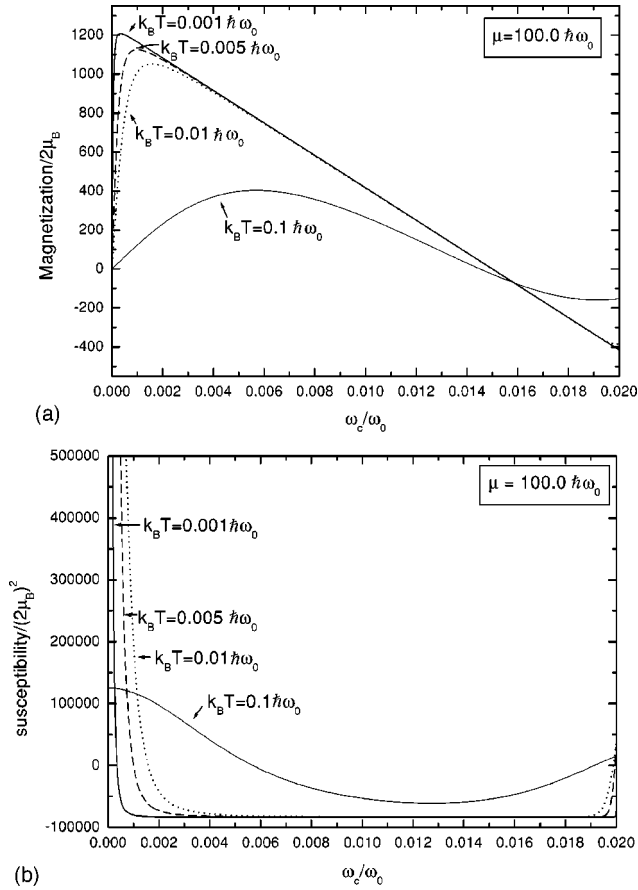


FIG. 4. Detailed plots of (a) magnetization and (b) susceptibility curves in a very weak magnetic-field regime. Temperature varies from $k_B T = 0.1 \hbar \omega_0$ to $k_B T = 0.001 \hbar \omega_0$ while the chemical potential μ is chosen as $100.0 \hbar \omega_0$. The system exhibits a paramagnetic behavior as ω_c / ω_0 is very near zero and turns to appear diamagnetic when the field becomes stronger. While the temperature approaches zero, the diamagnetic curve gives an asymptotic susceptibility which is about $-(\mu_B)^2 [\frac{1}{3}(\mu / \hbar \omega_0)^3 + \frac{1}{2}(\mu / \hbar \omega_0)^2]$.

2. Weak fields $\omega_c \ll \omega_0$

In this case the two characteristic frequencies and their ratios are approximated to

$$\omega_{\pm} \approx \omega_0 \left[1 \pm \frac{1}{2} \frac{\omega_c}{\omega_0} + \frac{1}{8} \left(\frac{\omega_c}{\omega_0} \right)^2 \right], \quad \frac{\omega_{\pm}}{\omega_{\mp}} \approx 1 \pm \frac{\omega_c}{\omega_0} + \frac{1}{2} \left(\frac{\omega_c}{\omega_0} \right)^2. \quad (5.4)$$

Now $\mathcal{M}_{\text{osc}}^-$ and $\mathcal{M}_{\text{osc}}^+$ have the same order of contribution due to the presence in their denominators of

$$[\sinh(2\pi^2 m k_B T / \hbar \omega_{\mp})]^2 \approx [\sinh(2\pi^2 m k_B T / \hbar \omega_0)]^2 \quad (5.5)$$

and of the strongly oscillating functions

$$[\sin(\pi m \omega_{\pm} / \omega_{\mp})]^2 \approx [\sin(\pi m \omega_c / \omega_0)]^2. \quad (5.6)$$

Consequently, the system is considered as lying in the mesoscopic phase. Similar conclusions can be reached for the behavior of the average electron number.

C. Intermediate temperatures: $\hbar \omega_- < k_B T < \hbar \omega_+$

These inequalities imply the constraint

$$\frac{\omega_c}{\omega_0} > \left| \frac{\hbar \omega_0}{k_B T} - \frac{k_B T}{\hbar \omega_0} \right|. \quad (5.7)$$

The weak-field case occurs only when $k_B T$ approaches $\hbar \omega_0$. In this case, one may think that the oscillatory terms $\mathcal{M}_{\text{osc}}^-$ and $\mathcal{M}_{\text{osc}}^+$ give their contribution to M as we have seen in the previous subsection. But, in fact, the hyperbolic sinus functions of the denominators have large arguments:

$$\sinh(2\pi^2 m k_B T / \hbar \omega_{\mp}) \approx \sinh(19.74m) \approx 0.5 \exp(19.74m),$$

and so overcomes the algebraic contribution of the sinus functions. The system hence goes to the Landau diamagnetic regime. On the other hand, for a strong field, we return to the approximation $M \approx 2\mu_B(\mathcal{M}_L + \mathcal{M}_{\text{osc}}^+)$ and the system shows the de Haas–van Alphen effect.

We have repeated in Fig. 2 the phase diagram of magnetization proposed by Ishikawa and Fukuyama. Let us however mention that the two intrinsic frequencies ω_{\pm} do not represent the exact borders between the different magnetic phases. In consequence this diagram should be taken in a qualitative sense only. In order to justify this, we choose the chemical potential equal to $100.0 \hbar \omega_0$ and make temperature vary through the different magnetic regimes. Figure 3(a) illustrates the weak-field regime. One can see that at low temperature $k_B T = 0.001 \hbar \omega_0$ the magnetization experiences strong fluctuations, called mesoscopic fluctuations. As T increases ($k_B T = 0.1 \hbar \omega_0$ and $k_B T = 0.5 \hbar \omega_0$), the strength of these fluctuations decreases. As the temperature gets higher (for example, $k_B T = 1.0 \hbar \omega_0$), the fluctuations disappear and we reach the Landau diamagnetism. In Fig. 3(b) the magnetic field lies between $1.9 \omega_0 mc/e$ and $3.1 \omega_0 mc/e$. When $k_B T = 0.01 \hbar \omega_0$, the system shows large fluctuations. One can see that if the magnetic field increases, the fluctuations diminish and the cycloidlike curve appears (de Haas–van Alphen oscillations). At higher temperature, e.g., $k_B T = 0.1 \hbar \omega_0$, one can see clearly that the mesoscopic fluctuations decrease and the phase turns almost to the de Haas–van Alphen oscillations. At, for example, $k_B T = 0.5 \hbar \omega_0$, the mixture of Landau diamagnetism and de Haas–van Alphen oscillations appears. If the temperature continues increasing (for example, $k_B T = 1.0 \hbar \omega_0$), the system will go from Landau diamagnetism to a mixture of Landau with de Haas–van Alphen. Figure 3(c) shows the de Haas–van Alphen phases. The position of the peak can be predicted from the simple formula

$$\frac{\omega_c}{\omega_0} = \frac{2\mu}{n\hbar\omega_0} - \frac{n\hbar\omega_0}{2\mu},$$

where n is some positive odd integer.

We also see that the de Haas–van Alphen oscillation is destroyed as the temperature increases. In Fig. 3(d) we see that at extreme low temperature ($k_B T = 0.001 \hbar \omega_0$), the curve shows many small fluctuations. This is an example of de Haas–van Alphen oscillations mixed with mesoscopic fluctuations.

Finally, we present in Figs. 4(a) and 4(b) a detail of the magnetization and the corresponding magnetic susceptibility $\chi = \partial M / \partial H$ in the region of very weak magnetic field. Temperatures are taken from $k_B T = 0.1 \hbar \omega_0$ to $0.001 \hbar \omega_0$ in order to show how the curves evolve. We notice that the system first exhibits a paramagnetic behavior all the more so since temperature and field are small. It turns to become diamagnetic while the strength of the magnetic field increases. The magnetic susceptibility in the latter region can be estimated to be $-(\mu_B)^2 [\frac{1}{3}(\mu/\hbar \omega_0)^3 + 1/2(\mu/\hbar \omega_0)^2]$.

VI. CONCLUSION

In this paper, we have established exact formulas for the thermodynamical potential of a two-dimensional gas of spinless electrons, confined in an isotropic harmonic potential, and submitted to a constant perpendicular magnetic field. From this it has become possible to study the magnetic moment and other thermodynamical quantities at different regimes of temperature and field. This exhaustive study was made possible thanks to the specific simplicity of the isotro-

pic harmonic potential. Of course, there exist other situations in which we could get similar exact expressions: anisotropic harmonic potential and harmonic groove, as indicated in Ref. 3. In the near future, we shall deal with less tractable but still integrable models (see, for instance, Ref. 6), such as infinite cylinder potential or quantum rings, cases in which expressing the trace (3.11) in a closed form is quite unexpected. We shall also explore the behavior, at different temperature and field regimes, of other thermodynamical quantities of current experimental interest, such as the heat capacity.⁷ Finally, we shall use coherent state techniques for a comprehensive investigation of the current density in the above model.

The authors are pleased to acknowledge Galliano Valent (LPTHE, Universities of Paris 6 and 7, France), Remi Mosseri (CNRS, GPS, Universities of Paris 6 and 7, France), Sorin Melinte (UPCPM, University of Louvain-la-Neuve, Belgium), and Yakov I. Granovskii (Szczecin University, Poland) for useful suggestions and comments. P.Y.H. is also grateful to the ICSC World Laboratory in Switzerland for financial support.

*Email address: gazeau@ccr.jussieu.fr

†Email address: hsiao@ccr.jussieu.fr

‡Email address: jellal@ictp.trieste.it, youpy.co.uk

¹Y. Ishikawa and H. Fukuyama, J. Phys. Soc. Jpn. **68**, 2405 (1999).

²V. Fock, Z. Phys. **47**, 446 (1928); C. G. Darwin, Proc. Cambridge Philos. Soc. **27**, 86 (1930).

³D. Yoshioka and H. Fukuyama, J. Phys. Soc. Jpn. **61**, 2368 (1992).

⁴K. Richter, D. Ullmo, and R. A. Jalabert, Phys. Rep. **276**, 1 (1996).

⁵M. Combescure and D. Robert, Rev. Math. Phys. **13**, 1055 (2001).

⁶R. Rosas, R. Riera, J. L. Marín, and H. León, Am. J. Phys. **68**, 835 (2000).

⁷V. Bayot, E. Grivei, S. Melinte, M. B. Santos, and M. Shayegan, Phys. Rev. Lett. **76**, 4584 (1996).